

High temperature ferromagnetism in $GdFe_2Zn_{20}$: large, local moments embedded in the nearly ferromagnetic Fermi liquid compound YFe_2Zn_{20} .

S. Jia¹, S. L. Bud'ko¹, G. D. Samolyuk², P. C. Canfield¹

¹Ames Laboratory US DOE and Department of Physics and Astronomy,
Iowa State University, Ames, IA 50011

²Ames Laboratory US DOE and Department of Chemistry,
Iowa State University, Ames, IA 50011

(Dated: May 16, 2021)

Abstract

The RFe_2Zn_{20} series manifests strongly correlated electron behavior for the non-magnetic $R = Y$ member and remarkably high temperature, ferromagnetic ordering ($T_C = 86$ K) for the local moment bearing $R = Gd$ member (a compound that is less than 5% atomic Gd). In contrast, the isostructural RCO_2Zn_{20} series manifests a more typical ordering temperature ($T_N = 5.7$ K for $GdCO_2Zn_{20}$) and YCO_2Zn_{20} does not show signs of correlated electron behavior. Studies of $R(Fe_xCo_{1-x})_2Zn_{20}$ ($R = Gd, Y$), combined with bandstructure calculations for the end members, reveal that YFe_2Zn_{20} is a nearly ferromagnetic Fermi liquid and that the remarkably high T_C associated with $GdFe_2Zn_{20}$ is the result of submerging a large local moment into such a highly polarizable matrix. These results indicate that the RFe_2Zn_{20} series, and more broadly the RT_2Zn_{20} ($T = Fe, Co, Ni, Mn, Ru, Rh, Os, Ir, Pt$) isostructural family of compounds, offer an exceptionally promising phase space for the study of the interaction between local moment and correlated electron effects near the dilute R limit.

PACS numbers: 75.20.Hr, 75.30.Mb, 75.50.Cc

The field of condensed matter physics has been interested in the effects of electron correlations from its inception^{1,2}. To this day, the properties of elemental Fe as well as Pd continue to present problems that interest both experimentalists as well as theorists³. In particular materials such as Pd or Pt, that are just under the Stoner limit (often referred to as nearly ferromagnetic Fermi liquids), or materials just over the Stoner limit, such as $ZrZn_2$ or Sc_3In on the ferromagnetic side, are of particular interest^{1,2,3}. Of even greater interest are new examples of nearly ferromagnetic Fermi liquids that can be tuned with a greater degree of ease than the pure elements: i.e. can accommodate controlled substitutions on a number of unique crystallographic sites in a manner that allows for (i) a tuning of the band filling / Fermi surface and (ii) the introduction of local moment bearing ions onto a unique crystallographic site. Such a versatile system would open the field to a greater range of experimental studies of strongly correlated electronic states as well as potentially allow for more detailed studies of quantum criticality and possibly even novel superconducting states.

In this letter we present our first results of an extensive study of the dilute, rare earth bearing, intermetallic series RT_2Zn_{20} (R = rare earth and T = transition metal) which supports a wide range of R ions for T in and near the Fe, Co and Ni columns of the periodic table. In particular, in this letter we will show how YFe_2Zn_{20} is an archetypical example of a nearly ferromagnetic Fermi liquid and how, by embedding Gd ions into this highly polarizable medium, $GdFe_2Zn_{20}$ can have a remarkably high ferromagnetic ordering temperature of 86 K, even though it contains less than 5% atomic Gd and the Fe is not moment bearing in the paramagnetic state.

The RT_2Zn_{20} series of compounds was discovered in 1997 by Nasch et al.⁴ and is isostructural to the cubic $CeCr_2Al_{20}$ structure ($Fm\bar{3}m$ space group)^{5,6}. The rare earth and transition metal ions each occupy their own single, unique crystallographic sites (8a and 16d respectively) whereas the Zn ions have three unique crystallographic sites (96g, 48f and 16c). In addition, the rare earth site is one of cubic point symmetry ($43m$). The coordination polyhedra for R and T are comprised fully of Zn, meaning that there are no $R-R$, $T-T$ or $R-T$ nearest neighbors and the shortest $R-R$ spacing is ≈ 6 Å. The lattice parameters for the series are ≈ 14 Å. Although the crystallography of this series was well detailed, there have been, to date, no measurements of these compounds' physical properties. This, to some extent, is not unexpected since the limited data sets available on the RT_2Al_{20} compounds^{6,7} indicated very low ordering temperatures, consistent with the very low R -concentrations.

Single crystals of $R\text{Fe}_2\text{Zn}_{20}$, $R\text{Co}_2\text{Zn}_{20}$ and $R(\text{Fe}_x\text{Co}_{1-x})_2\text{Zn}_{20}$ ($R = \text{Gd, Y}$) were grown from high temperature solutions⁸ rich in Zn using initial compositions of $R_2\text{T}_4\text{Zn}_{94}$. The constituent elements were placed in an alumina crucible, sealed in a quartz ampule under 1=3 atmosphere Ar and heated in a box furnace to 1000 °C and then slowly cooled to 600 °C over up to 100 hours. The resulting single crystals were large and often manifested clear [111] facets (see the inset to Figure 2a below). For $R(\text{Fe}_x\text{Co}_{1-x})_2\text{Zn}_{20}$, x values are nominal values, but these are confirmed by elemental analysis as well as compliance with Vegard's law, with the lattice parameter varying linearly between the $x = 0$ and $x = 1$ end points. Field and temperature dependent magnetization measurements were made using Quantum Design MPMS units whereas transport and specific heat measurements were made using Quantum Design PPMS units with ³He options. The electronic band structure was calculated using the atomic sphere approximation tight binding linear muffin-tin orbital (TB-LMTO-ASA) method^{9,10} within the local density approximation (LDA) with Barth-Hedin¹¹ exchange-correlation using the experimental values of the lattice parameters. The number of atoms in the reduced unit cell is 46. A mesh of 16 k points in the irreducible part of the Brillouin zone (BZ) was used. The 4f-electrons of Gd and Lu atoms were treated as core states (polarized in the case of Gd atoms).

Figures 1 and 2 present the temperature dependent electrical resistivity, specific heat and low field magnetization data, as well as anisotropic $M(H)$ data, for $\text{GdFe}_2\text{Zn}_{20}$ and $\text{GdCo}_2\text{Zn}_{20}$. There are two conspicuous differences between the physical properties of these compounds: (i) $\text{GdFe}_2\text{Zn}_{20}$ orders ferromagnetically whereas $\text{GdCo}_2\text{Zn}_{20}$ orders antiferromagnetically, and (ii) $\text{GdFe}_2\text{Zn}_{20}$ orders at a remarkably high temperature of $T_C = 86$ K whereas $\text{GdCo}_2\text{Zn}_{20}$ orders at the more representative $T_N = 5.7$ K. From Figure 2a the high temperature Curie constant can be determined, giving effective moments ($8.05 \mu_B$ and $8.15 \mu_B$ for $T = \text{Fe}$ and $T = \text{Co}$ respectively) consistent with the effective moment of Gd^{3+} , indicating that, in the paramagnetic state, there is little or no contribution from the transition metal. The saturated moment deduced from the data in Figure 2b is close to that associated with Gd^{3+} ; slightly lower for $\text{GdFe}_2\text{Zn}_{20}$ and slightly higher for $\text{GdCo}_2\text{Zn}_{20}$. The magnetic entropy associated with each phase transitions is approximately $R \ln 8$, with more uncertainty associated with the subtraction of the $\text{Y T}_2\text{Zn}_{20}$ data for $T = \text{Fe}$ than for $T = \text{Co}$ due to much higher ordering temperature. The remarkably high ordering temperature found for $\text{GdFe}_2\text{Zn}_{20}$ is not unique to the $R = \text{Gd}$ member of the $R\text{Fe}_2\text{Zn}_{20}$ series. For $R =$

Gd-Tm transitions to ferromagnetically ordered states occur at temperatures that roughly scale with the de Gennes parameter.¹²

In order to better understand this conspicuous difference in ordering temperatures, band-structural calculations were carried out. Figure 3 presents the density of states as a function of energy for both LuFe₂Zn₂₀ and LuCo₂Zn₂₀. The upper curve in each panel is the total density of states whereas the lower curve is the density of states associated with the transition metal ion. It should be noted that the difference between LuFe₂Zn₂₀ and LuCo₂Zn₂₀ density of states can be rationalized in terms of the rigid band approximation, with the Fermi level for LuCo₂Zn₂₀ being 0.3 eV higher than that for LuFe₂Zn₂₀, associated with the two extra electrons per formula unit. Calculations done on YFe₂Zn₂₀ and GdFe₂Zn₂₀ as well as on YCo₂Zn₂₀ and GdCo₂Zn₂₀ lead to similar density of states curves¹² and further analysis of the GdFe₂Zn₂₀ and GdCo₂Zn₂₀ bandstructural results leads to the prediction that for GdFe₂Zn₂₀ the ground state will be ferromagnetic with a total saturated moment of approximately 6.8 μ_B (with a small induced moment on the Fe opposing the Gd moment) and for GdCo₂Zn₂₀ the ground state will be antiferromagnetic with a saturated moment of 7.15 μ_B (and practically no induced moment on Co). These results are consistent with the saturated values of the magnetization seen in Fig. 2b.

These calculations indicate that the RFe₂Zn₂₀ compounds should manifest a higher $N(E_F)$ than the RCo₂Zn₂₀ analogues and bring up the question of whether or not this is the primary reason for the remarkably high T_C found for GdFe₂Zn₂₀. In addition they bring up the question of how correlated the electronic state is in the nominally non-magnetic Lu- or Y-based analogues. In order to address these questions two substitutional series were grown: Y(Fe_xCo_{1-x})₂Zn₂₀ and Gd(Fe_xCo_{1-x})₂Zn₂₀. Figure 4 presents thermodynamic data taken on the Y(Fe_xCo_{1-x})₂Zn₂₀ series. For $x = 0$ the low temperature, linear component of the specific heat (γ) is relatively small (19 mJ/m³K²) and the susceptibility is weakly paramagnetic and essentially temperature independent. As x is increased there is a monotonic (but clearly super-linear) increase in the samples' paramagnetism as well as, for larger x -values, an increase in the low temperature γ values. For YFe₂Zn₂₀ ($x = 1$) the value of γ has increased to over 250% of that for YCo₂Zn₂₀ and the susceptibility has become both large and temperature dependent. Figure 5 presents data on the analogous Gd(Fe_xCo_{1-x})₂Zn₂₀ series. As x is increased the ground state rapidly becomes ferromagnetic and the transition temperature increases monotonically (but again in a super-linear fashion) and the high field,

saturated, magnetization decreases weakly, in a monotonic fashion.

Taken together, figures 4 and 5 demonstrate a clear correlation between x , the linear component of the electronic specific heat, the enhanced magnetic susceptibility of the Y-based series and the Curie temperature and the saturated magnetization of the Gd-based series. This correlation can be more clearly seen if the relation between the linear component of the specific heat and the low temperature susceptibility of the Y-based series is placed in the context of a nearly ferromagnetic Fermi liquid: i.e. if the Stoner enhancement parameter, Z , for each member of the series can be determined.¹³ For such systems the static susceptibility (corrected for the core diamagnetism¹⁴) is $\chi = \chi_0 / (1 - Z)$, where $\chi_0 = \mu_B N(E_F)$ is the Pauli paramagnetism. Given that the linear component of the specific heat is given by $\gamma_0 = (k_B)^2 N(E_F) / 3$, if both the low temperature specific heat and magnetic susceptibility can be measured, then the parameter Z can be deduced, ($Z = 1 - (3 \gamma_0^2 / k_B^2) (\chi_0 = \chi_0)$). The canonical example of such a system is elemental Pd for which, using data from ref. 15, $Z = 0.83$. For YFe_2Zn_{20} , $Z = 0.89$, a value that places it even closer to the Stoner limit than Pd. It should be noted that the temperature dependent susceptibility of YFe_2Zn_{20} is remarkably similar to that of Pd as well (see ref. 3 and references therein). The x -dependence of the experimentally determined values of χ and γ ($T = 0$), as well as the inferred value of Z , for the $Y(Fe_xCo_{1-x})_2Zn_{20}$ series are plotted in Fig. 6a. By choosing x , $Y(Fe_xCo_{1-x})_2Zn_{20}$ can be tuned from being exceptionally close to the Stoner limit to well removed from it. Corrections to these inferred Z values coming from the difference between the measured electronic specific heat coefficient, γ , and Sommerfeld coefficient, γ_0 , where $\gamma = \gamma_0(1 + \lambda)$ only serve to slightly increase Z since λ , the electron mass enhancement parameter, is positive definite. We can estimate $\lambda = 0.85$ and 0.22 , for $x = 1$ and $x = 0$ respectively, and this shifts Z to 0.94 for YFe_2Zn_{20} and to 0.50 for YCo_2Zn_{20} .

When the non-magnetic Y ion is replaced by the large, Heisenberg moment associated with the $S = 7/2$ Gd³⁺ ion, as x is varied from zero to one in the Gd(Fe_xCo_{1-x})₂Zn₂₀ series, the Gd local moments will be in an increasingly polarizable matrix, one that is becoming a nearly ferromagnetic Fermi liquid. This results in an increasingly strong coupling between the Gd local moments as x is increased. Figure 6b plots the x -dependence of T_C and χ_{sat} for the Gd(Fe_xCo_{1-x})₂Zn₂₀. The value of T_C increases in a monotonic but highly non-linear fashion in a manner reminiscent to the behavior associated with the increasing polarizability of $Y(Fe_xCo_{1-x})_2Zn_{20}$ seen in figure 6a. The χ_{sat} value for the field applied

along the [111] direction varies systematically from the slightly enhanced $7.3 \mu_B$ value found for $GdCo_2Zn_{20}$ to the slightly deficient value of $6.5 \mu_B$ found for $GdFe_2Zn_{20}$.

In addition to x -dependence, this conceptually simple and compelling framework can also be used to understand the rather curious temperature dependence of the χ vs. T data for $GdFe_2Zn_{20}$ seen in Fig. 2a. As T is decreased the electronic background that the Gd^{3+} ion is immersed in becomes increasingly polarizable (as shown in Fig. 4a for $x = 1$), leading to a temperature dependent coupling that in turn leads to the non-linearity of the χ vs. T data. If a constant effective moment for the Gd^{3+} is assumed, then a temperature dependent paramagnetic χ can be extracted from the data in Fig. 2a: $\chi(T) = \chi_0 + C/(T + \theta)$. This temperature dependent χ , shown in Fig. 4a, tracks the electronic susceptibility of the YFe_2Zn_{20} remarkably well, both increasing by ~ 1.7 upon cooling from 300 K to 100 K.

One consequence of placing Gd ions into a matrix so close to the Stoner limit is an enhanced sensitivity to small sample-to-sample variations. This is most clearly illustrated by the data for the $Gd(Fe_{0.88}Co_{0.12})_2Zn_{20}$ samples shown in Figs. 5a and 6b. Although the samples have the same nominal composition there is a clear difference in their transition temperatures (Fig. 5a). This difference though is not too significant given the large dT_C/dx slope seen in Fig. 6b. On the other hand, measurements on four separate samples of $Gd(Fe_{0.25}Co_{0.75})_2Zn_{20}$ did not show any significant variations in T_C . Such sensitivity of correlated electron states to small disorder is not uncommon, giving rise to significant variation in measured T_C for samples of Sc_3In and $ZrZn_2$ [1,16] as well as dramatic changes in the transport properties of heavy fermions such as $YbNi_2B_2C$.¹⁷

In summary, the $R(Fe_xCo_{1-x})_2Zn_{20}$ series offers a unique opportunity to systematically study the evolution of a nearly ferromagnetic Fermi liquid (for $R = Y, Lu$) and also offers the possibility of studying the effects that such a polarizable background has on the ordering of large local moments which are located on an existing, unique crystallographic site. The broader RT_2Zn_{20} family of compounds offers an even larger phase space for the study of correlated electron physics (for $T = Fe, Ru, Os$ as well as for $R = Yb$ and Ce)^{12,18} and for the study of local moment physics, all in the limit of a dilute, rare earth bearing, intermetallic series. The study of these compounds promises to be a fruitful new phase space for several years to come.

Acknowledgments

We are indebted to the following students and magneticians: K. Dennis, N. Ni, J. Friedrich, S.A. Law, H. Ko, E.D. Mun, A. Safa-Sefat for help in samples' growth and characterization and to J. Schmalian and B.N. Harmon for useful discussions. Ames Laboratory is operated for the U.S. Department of Energy by Iowa State University under Contract No. W-7405-Eng-82. This work was supported by the Director for Energy Research, Office of Basic Energy Sciences.

-
- ¹ T. Moriya, Spin fluctuations in itinerant electron magnetism (Springer, Berlin, 1985).
 - ² P.E. Brommer, and J.J.M. Franse, in: Ferromagnetic Materials, Vol. 5, edited by K.H.J. Buschow and E.P. Wohlfarth (Elsevier, Amsterdam, 1990) p.224.
 - ³ B. Zeller, A. Paintner, and J. Voitlander, J. Phys.: Cond. Mat. 16 (2004) 919.
 - ⁴ T. Nasch, W. Jeitschko, and U.C. Rodewald, Zeitschrift für Naturforschung, B: Chem. Sciences 52 (1997) 1023.
 - ⁵ P.I. Kripyakevich, and O.S. Zarechnyuk, Dopov. Akad. Nauk Ukr. RSR, Ser. A 30 (1968) 364.
 - ⁶ V.M.T. Thiede, W. Jeitschko, S. Niemann, and T. Ebel, J. Alloys Compd. 267 (1998) 23.
 - ⁷ O.M. Oze, L.D. Tung, J.J.M. Franse and K.H.J. Buschow, J. Alloys Compd. 268 (1998) 39.
 - ⁸ P.C. Caneld and Z. Fisk, Phil. Mag. B 65 (1992) 1117.
 - ⁹ O.K. Andersen, Phys. Rev. B 12 (1975) 3060.
 - ¹⁰ O.K. Andersen, O. Jepsen, Phys. Rev. Lett. 53 (1984) 2571.
 - ¹¹ U. von Barth, L. Hedin, J. Phys. C 5 (1972) 1629.
 - ¹² S. Jia, et al., unpublished.
 - ¹³ J.E. Ziman, Principles of the theory of solids, 2nd edition (Cambridge University Press, Cambridge, 1972).
 - ¹⁴ Using Table 5.7 (p. 306) in L.N. Mulay, E.A. Boudreaux Theory and applications of molecular diamagnetism (John Wiley & Sons, NY 1976) we can estimate the core diamagnetism of $Y(Fe_xCo_{1-x})_2Zn_{20}$ to be $2.3 \cdot 10^4$ emu/mol.
 - ¹⁵ G. Chouteau, R. Fournieux, K. Gobrecht, and R. Tournier, Phys. Rev. Lett. 20 (1968) 193.
 - ¹⁶ J. Fluquet, et al., private communication.

- ¹⁷ M . A . Avila, S . L . Bud'ko, and P . C . Can eld Phys. Rev. B 66 (2002) 132504; M . A . Avila, Y . Q . Wu, C . L . Condron, S . L . Bud'ko, M . K ram er, G . J . M iller, and P . C . Can eld Phys. Rev. B 69 (2004) 205107; S . L . Bud'ko and P . C . Can eld Phys. Rev. B 71 (2005) 024409.
- ¹⁸ M . S . Torikachvili, S . Jia, S . T . Hannahs, R . C . Black, W . K . Neils, D inesh M artien, S . L . Bud'ko, and P . C . Can eld, cond-m at/0608422.

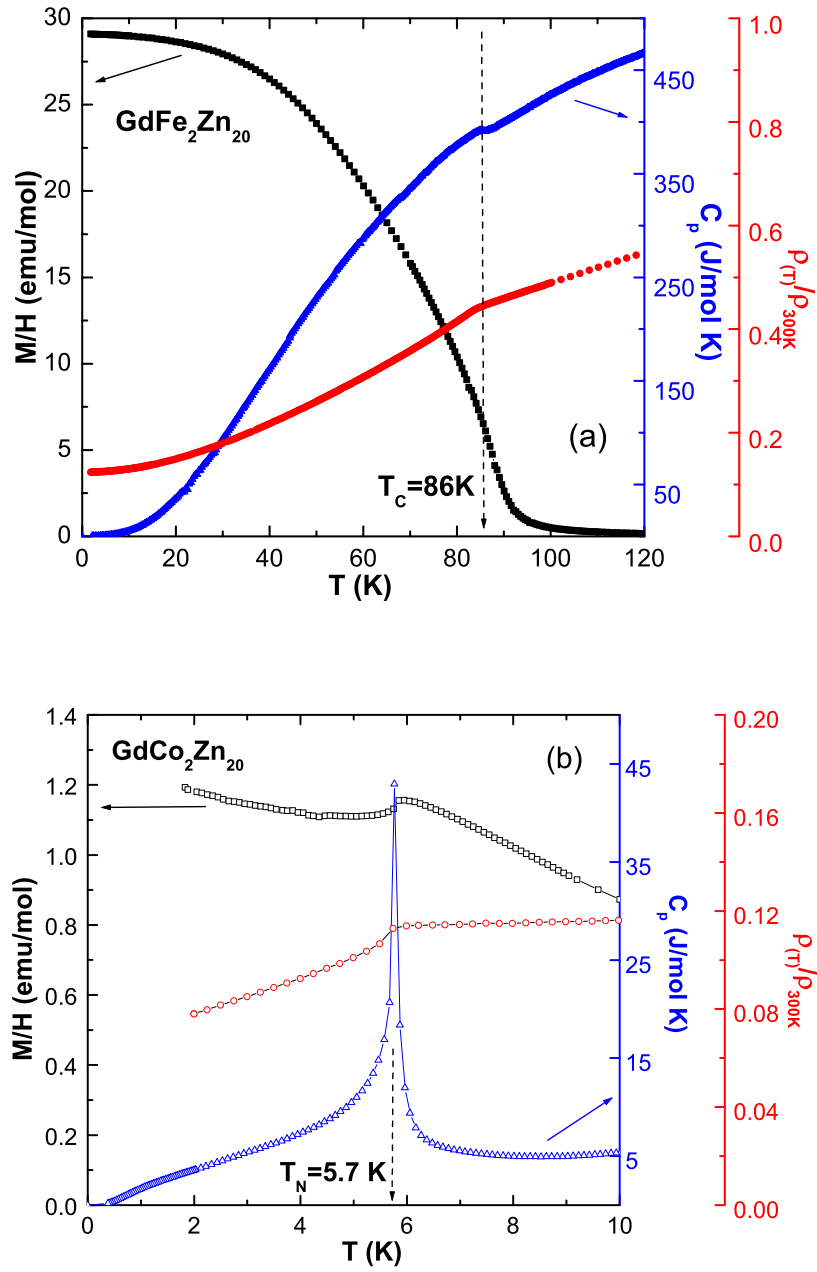


FIG. 1: Temperature dependent specific heat, resistivity, and low field ($H = 1000$ Oe) magnetization divided by field for (a) GdFe₂Zn₂₀ and (b) GdCo₂Zn₂₀. For GdFe₂Zn₂₀ $\rho(300K) = 73$ $\mu\Omega$ cm and for GdCo₂Zn₂₀ $\rho(300K) = 60$ $\mu\Omega$ cm.

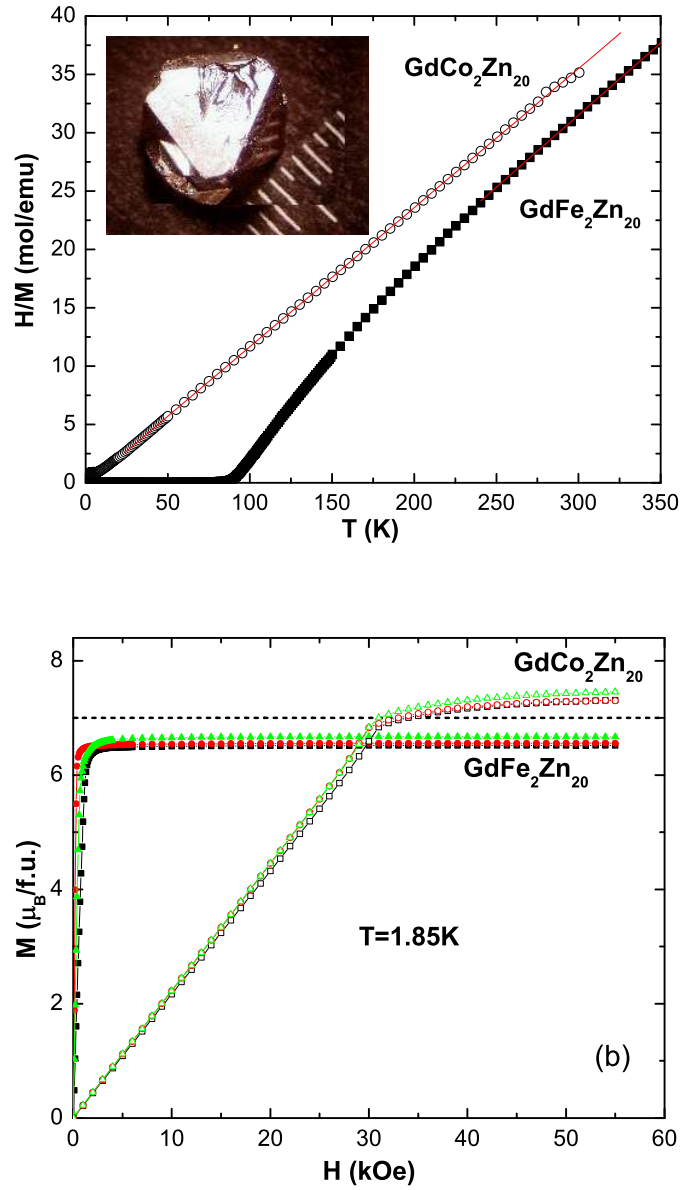


FIG. 2: (a) H/M as a function of T for $\text{GdFe}_2\text{Zn}_{20}$ and $\text{GdCo}_2\text{Zn}_{20}$ (dotted lines show region used for the high temperature Curie-Weiss fit). (b) Anisotropic $M(H)$ ($T = 1.85\text{ K}$) for $\text{GdFe}_2\text{Zn}_{20}$ and $\text{GdCo}_2\text{Zn}_{20}$. For each sample measurements for $H \parallel [100]$, $H \parallel [110]$, and $H \parallel [111]$ are shown. Inset to figure 2a: a single crystal of $\text{YFe}_2\text{Zn}_{20}$ next to a mm scale.

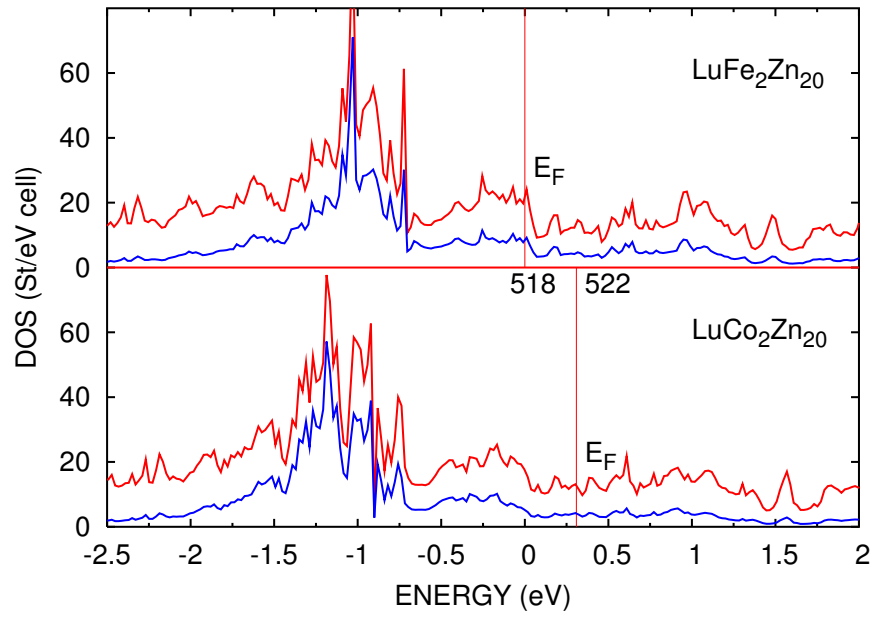


FIG .3: Density of states as a function of energy for LuFe₂Zn₂₀ and LuCo₂Zn₂₀. The upper curve is total density whereas the lower curve is partial density of states associated with Fe or Co.

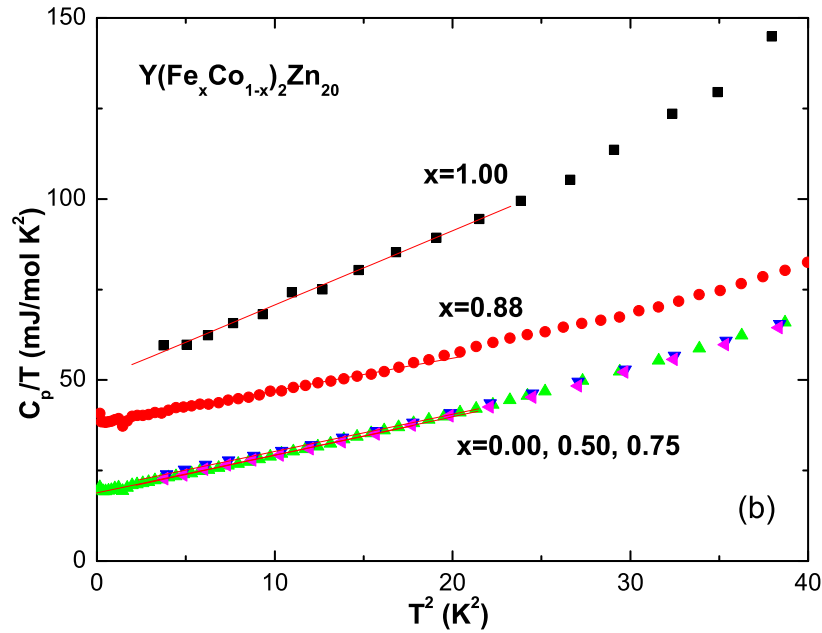
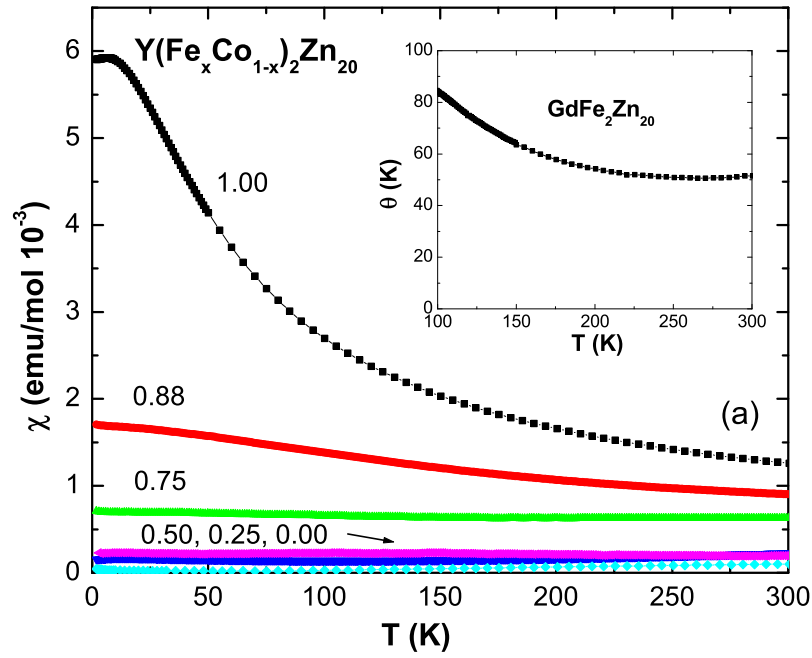


FIG .4: Temperature dependent magnetic susceptibility (a) and low temperature C_p/T as a function of T^2 (b) for $\text{Y}(\text{Fe}_x\text{Co}_{1-x})_2\text{Zn}_{20}$ series. Inset to figure 4a: temperature dependence of paramagnetic Curie temperature for $\text{GdFe}_2\text{Zn}_{20}$ (see text).

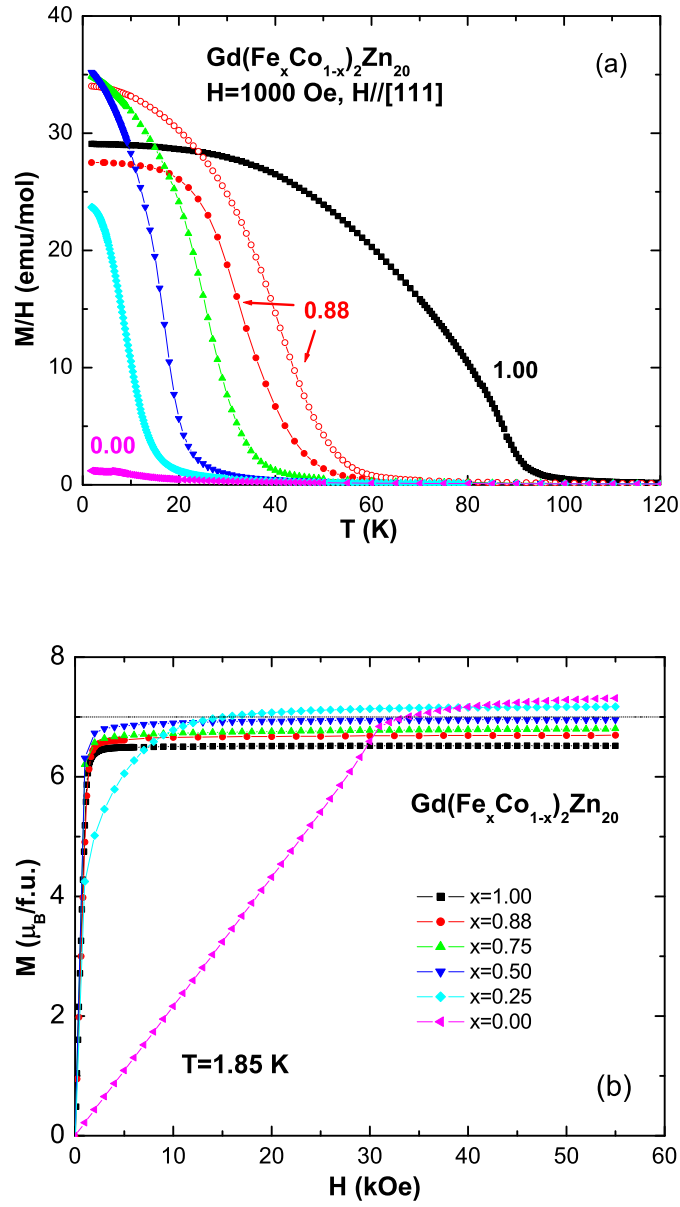


FIG. 5: Low field magnetization divided by field as a function of temperature for $x = 1.00, 0.88, 0.75, 0.50, 0.25,$ and 0.00 – from right to left (a) and low temperature ($T = 1.85$ K) magnetization as a function of applied field (b) for $\text{Gd}(\text{Fe}_x\text{Co}_{1-x})_2\text{Zn}_{20}$ series. Note that in (a) data from two samples of $x = 0.88$ are shown.

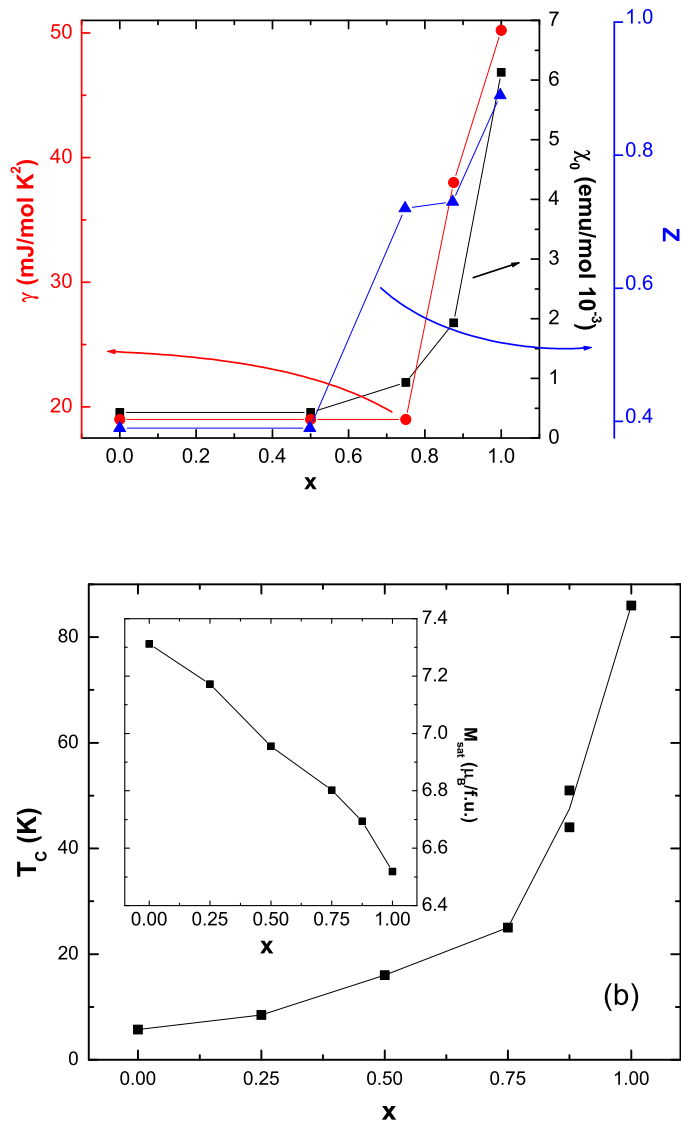


FIG. 6: Plots of linear coefficient of the specific heat, γ , magnetic susceptibility for $T \neq 0$ corrected for core diamagnetism¹⁴, χ_0 , and Stoner enhancement factor, Z , for $\text{Y}(\text{Fe}_x\text{Co}_{1-x})_2\text{Zn}_{20}$ series (a) and T_C for $\text{Gd}(\text{Fe}_x\text{Co}_{1-x})_2\text{Zn}_{20}$ series (b). Inset to (b) shows M_{sat} as a function of x for $\text{Gd}(\text{Fe}_x\text{Co}_{1-x})_2\text{Zn}_{20}$ series.